

# A Study of the Ten-Lump Kinetic Model in the Fluid Catalytic Cracking Unit Using COMSOL Multiphysics

**Digieneni Yousuo**

A lecturer and a Petrochemical Engineer

Department of Chemical Engineering, Niger Delta University, P.O.BOX 071  
Yenagoa, Bayelsa State of Nigeria

## Abstract

*The COMSOL Multiphysics Computational Fluid Dynamics (CFD) software was used to simulate the Fluid Catalytic Cracking (FCC) riser reactor. The ten-lump kinetic model was used to describe the kinetics of the reactions in the reactor. The extra fine mesh generator was employed to produce grid refinement in the riser reactor which ensured a better prediction of the hydrodynamics of riser reactor in the Fluid Catalytic Cracking Unit (FCCU). The reactor riser of the Port Harcourt Refinery Company (PHRC) was used as a case study. The riser reactor was meshed into 77, 358 elements and simulation was carried out. The distributions of pressure, velocity, temperature and products yields were obtained. The predicted values were compared with practical values from Port Harcourt Refinery Company plant and they were in good agreement.*

**Key words:** COMSOL Multiphysics, Computational Fluid Dynamics, Fluid Catalytic Cracking Unit, Riser Reactor, Kinetic Model, Reactions, Lumping Schemes, Product Yields

## 1. Introduction

Modern refinery has many units. Fluid catalytic cracking (FCC) unit is one of them and it is the workhorse of modern refinery. The FCC reactor is one of the most complex equipment in the refinery. There are several types of this in the fluid catalytic cracking unit (FCCU). Each type has several parts and is equipped with several internals such as cyclone separators and baffles. Most of the reactions in the FCC reactor occur in the FCC riser reactor. Many complicated processes such as catalytic cracking, fluid flow, heat and mass transfer are involved in the FCCU. The equations governing the fluid flow problems are a system of coupled non-linear partial differential equations (PDEs). Analytic methods can yield very few solutions. Numerical methods are frequently employed (Rajkumar et al., 2005; Ying et al., 2006; Idris et al., 2007; Versteeg and Malalasekera, 2007). The use of CFD technique in predicting or simulating a complex refinery process will provide an in-depth understanding of the processes in this equipment, assist to solve processing and operating problems, design of new units and scaling up of pilots plants.

This study uses COMSOL Multiphysics CFD software for the simulation of the FCC reactor riser.

## 2. Methodology

### 2.1 The riser kinetic model

The modelling is based on the schematic flow diagram of the PHRC FCCU reactor presented in Figure 1 and the PHRC FCCU riser reactor in Figure 2. The riser reactor is 33m long and the diameter is 0.8m and other details may be found in Yousuo and Ogbeide (2015). The FCCU reactor consists of the riser reactor, reactor catalyst stripper, reactor separator or disengager, reactor cyclones and other equipments. To have acceptable predicted results between kinetics and applicability of the COMSOL Multiphysics CFD software, the ten lump kinetic schemes was considered for predicting the behaviour of the riser reactor as shown in figure 3. The lumps for the 10- lump kinetic scheme are the heavy fuel oils from the paraffins ( $HFO_{ph}$ ), the heavy fuel oils from the Naphtenes ( $HFO_{Nh}$ ), the heavy fuel oils from the aromatic substituent groups ( $HFO_{Ah}$ ), the heavy fuel oils of the carbons among the aromatic rings( $HFO_{Rh}$ ), the light fuel oils from the paraffins ( $LFO_{ph}$ ), the light fuel oils from the Naphtenes ( $LFO_{Nh}$ ), the light fuel oils from the aromatic substituent groups ( $LFO_{Ah}$ ), the light fuel oils of the carbons among the aromatic rings ( $LFO_{Rh}$ ), gasoline (G) and COKE (C).

In this model COKE (C) represents 50% coke and 50% C<sub>1</sub>-C<sub>4</sub> gases. The rate expressions of the 10-lump kinetic scheme and other details are shown elsewhere (Jacob et al, 1976).

## 2.2 Plug-flow reactor equations

The reactor model is an ideal plug-flow reactor, described by the mass balance in equation (1). Assuming constant reactor cross section and flow velocity, the species concentration gradient as fraction of residence time ( $\tau$ ) is given in equation (2). The reaction rates are given by  $r_j = K_j C_i$  and to account for the different time scales, two different activity functions are used. For the non-coking reactions the activity function is given in equation (3).

$$\frac{dF_i}{dV} = \sum_j V_{ij} r_j = R_i \quad (1)$$

$$\frac{dF_i}{dV} = \frac{d(V C_i)}{dV} = \frac{dC_i}{d\tau} = R_i \quad (2)$$

$$a = e^{-k_d C_c} \quad (3)$$

The reaction rates are modified by the activity according to equation (4). For the coking reactions, the activity function is given by equation (5) where  $\alpha$  is a deactivation constant depending on the residence time. The modified reaction rates are given by equation (6). The coke content is given by equation (7) and equation (8). The values of  $a$ ,  $b$ ,  $\phi$  and  $\alpha$  are obtained from (Rajkumar et al., 2005; Jafar et al., 2008 and Yousuo, 2014) as shown in equation (9) and (10) respectively.

$$r_j = a K_j C_i \quad j = 1, 2, 3, 4, 5, 6, 7, 8, 13, 14, 15 \quad (4)$$

$$b = e^{-\psi t} = e^{-\alpha t} \quad (5)$$

$$r_j = b K_j C_i \quad j = 9, 10, 11, 12, 16, 17, 18, 19, 20 \quad (6)$$

$$C_c = 2.43 \times 10^{-3} t_c^{0.2} \quad (7)$$

$$Q(C_c) = \frac{1}{1 + 69.47(100C_c)^{3.8}} \quad (8)$$

$$\phi = \exp(-\alpha t_c) \quad (9)$$

$$\alpha = \alpha_0 \exp\left(\frac{-E}{RT}\right) \quad (10)$$

**For the mass transport**, the inlet and outlet concentrations are obtained from equation (11) and the velocity and pressure for ideal gases are obtained from equation (12) and (13) respectively. The static head of catalyst in the riser can be calculated using equation (14). The details on choosing the void fraction variable, assumed gas velocity, slip factor and the vapourisation heat of the feed in the riser inlet are shown elsewhere (Rajkumar et al., 2005 and Yousuo, 2014).

$$\text{Inlet: } c = c_{in}, \text{ Outlet: } c = c_{out} \quad (11)$$

$$v = \frac{R_g T}{p} \sum F_i \quad (12)$$

$$p = R_g T \sum C_i \quad (13)$$

$$-\frac{dp}{dz} = \rho_{cat} g (1 - \varepsilon) \quad (14)$$

**For momentum transport**, the inlet and outlet pressure are obtained from equation (15)

$$\text{Outlet: } p = p_{in} - \rho_{cat} g (1 - \varepsilon) (z - z_0) \quad (15)$$

**For energy balance**, neglecting pressure drop, the energy balance for an ideal reacting gas, as well as an incompressible reacting liquid is given by equation (16) and (17). The inlet temperature is calculated putting into consideration the energy balance of the components. Equation (18) is used in calculating the inlet temperature while equation (19) is used for calculating the outlet temperature.

$$\sum_i M_i C_{p,i} \frac{dT}{dV} = w_s + Q + Q_{ext} \quad (16)$$

$$Q = -\sum_j H_j r_j \quad (17)$$

At  $z = z_0 = 0$ ,  $w_s = 0$ ,  $Q_{ext} = 0$ , equation (16) and (17) becomes  $\sum_i M_i C_{p,i} \frac{dT}{dV} - Q = 0$

This implies that

$$M_{cat} \cdot C_{p,cat} \cdot (T - T_{cat}) + M_{go} \cdot C_{p,go}^l \cdot (T_{vap} - T_{go}) + M_{go} \cdot C_{p,go}^v \cdot (T - T_{vap}) + M_{go} \cdot \Delta H_{vap} + M_{ds} \cdot C_{p,ds} \cdot (T - T_{ds}) = 0$$

That is

$$T_0 = \frac{(M_{cat} C_{p,cat} T_{cat}) - (M_{GO} C_{p,GO}^l (T_{vap} - T_{GO})) + (M_{GO} C_{p,GO}^v T_{vap}) - (M_{GO} \Delta H_{vap}) - (M_{ds} C_{p,ds} T_{ds})}{M_{cat} C_{p,cat} + M_{GO} C_{p,GO}^v + M_{ds} C_{p,ds}} \quad (18)$$

At  $z = h$  or  $z$ ,  $w_s = 0$ ,  $Q_{ext} = 0$ , equation (16) and (17) becomes  $\sum_i M_i C_{p,i} \frac{dT}{dV} = Q$

$$\text{That is, } \sum_i M_i C_{p,i} \frac{dT}{dV} = -\sum_j H_j r_j$$

$$\text{This implies that } T_z - T_0 = -\frac{\sum_j H_j r_j}{\sum_i M_i C_{p,i}} dv = -\frac{\sum_j H_j r_j}{\sum_i M_i C_{p,i}} (\pi D)(z - z_0)$$

$$\text{That is, } T_z = T_0 - \frac{\pi D \sum_j H_j r_j}{\sum_i M_i C_{p,i}} z$$

$$\text{By our correlation } T_z = T_0 - \frac{\pi D \sum_j H_j r_j}{\sum_i M_i C_{p,i}} z \text{ is}$$

$$T_z = T_0 - 0.55 * z \text{ or } T_0 - 7.7 * t^{0.35} \quad \text{hence}$$

$$\text{Outlet: } T = T_z = T_0 - 7.7 * t^{0.35} \quad (19)$$

### 2.3 Boundary conditions

The boundary conditions for the riser reactor are shown in table1.

## 3 Materials, Mesh generation and Simulation

### 3.1 Materials

The average molecular weight, the thermodynamic properties of the feed, the plant operating conditions and the properties of the catalyst used in this study, the specific heat of different lumps and the kinetic parameters for cracking reactions are shown in table 2 to 6 and others are found elsewhere (PHRC, 1987; Rajkumar et al., 2005 and Jafar et al., 2008).

### 3.2 Mesh generation and Simulation

The extra fine mesh generator of the COMSOL Multiphysics software was used to produce grid refinement in the riser reactor. The riser reactor was meshed into 77, 358 triangular elements. Figure 3 shows the computational grid used to represent the computational domain of the riser reactor. The simulations in this work used the 3-dimensional model of the COMSOL multiphysics CFD software in a windows vista™ Home Premium; model: HP Pavilion dv 6500 Notebook PC, Processor: Intel (R) Core(TM)2 Duo CPU T5450 @ 1.66GHz - 1.67GHz, Memory (Ram): 250GB and System type: 32-bit operatin system.

## 4.0 Results and discussion

### 4.1 The riser reactor hydrodynamics

Figures 5, 6 and 7 shows the velocity profile in the reactor riser, the surface velocity at the input of the riser and the surface velocity at the output of the riser respectively. The figures show that the velocity at the center of the riser is higher than the velocity near the walls of the riser. This is due to viscosity, shear and frictional forces at the walls of the riser.

Figure 8 shows the pressure profile in the reactor riser. The figure visibly indicates a decrease of pressure from the inlet (16570pa) to the outlet (94080pa) of the riser. Figure 9 shows the pressure distribution along the riser in the x-y coordinates for the pressure head using PHRC plant parameters. The decrease was as a result of the acceleration due to gravity on the mixture and other viscosity, shear and frictional forces at the walls of the riser.

Figures 10 and 11 show the temperature profile and temperature in the reactor riser. Gas oil/heavy diesel oil, medium pressure steam and fresh catalyst enter the reactor riser at a temperature of 505K, 464K and 1004K respectively. The medium pressure steam atomises the gas oil/heavy diesel oil as they travel up along the reactor riser increasing catalysis and the rate of reaction. The hydrocarbons and catalyst mixture travel upwards and the temperature inside the FCC riser decreases because of the endothermic cracking reactions. The mixture temperature of the riser falls sharply to 803K for PHRC plant because sensible heat of catalyst coming from the regenerator is utilized in providing heat for raising the sensible heat of feed, for vapourising the feed, and for further heating of the vapourised feed.

#### 4.2 The effect of the c/o ratio on the reactor riser performance (10-lump model)

The catalyst oil ratio (COR) is very important parameter in FCC process. The gasoline yield increases with the increasing C/O ratio (Figure 12). Hold up of catalyst (1- $\epsilon$ ) increased with increase of COR, so for all investigated input catalyst temperature (Figure 13), the increase of hold up can lead to higher conversion and pressure drop (Figure 14).

#### 4.3 Yield in the riser

Figure 15 shows the yield in the reactor riser versus the axial distance.  $HFO_{Ph}$ ,  $HFO_{Nh}$  and  $HFO_{Ah}$  and  $HFO_{Rh}$  are broken down and as a result their weight fraction decreased along the riser reactor from the inlet to the outlet.  $LFO_{Pl}$ ,  $LFO_{Nl}$ ,  $LFO_{Al}$  and  $LFO_{Rl}$  are formed and later broken down to  $G$  and  $C$  lumps. Table 7 shows the predictions of this work which were compared with PHRC plant data. According to table 7, a good agreement between the plant data and this model prediction was observed. The major source of discrepancy (deviation) is attributed to the kinetic parameters. This is because the weakness of lumping methodology for catalytic cracking reaction is that the kinetic constants are a function of the feed stock properties and the catalyst type.

### 5. Conclusion

A practical riser reactor of the FCCU has been simulated using COMSOL Multiphysics CFD software. The 10-lump kinetic model was used to describe the reactions taking place in the riser reactor.

The effect of the operating conditions on the system behaviour has also been studied. The model predictions of the gas oil conversion, product yield, were validated by comparison with PHRC plant. The model helps us get good insight into the performance of an industrial riser reactor that would be useful for optimization of fluid catalytic cracking.

### References

- Idris M.N., Mahmud T. and Gibbs B. (2007), "Application of process hydrodynamics Design of a Robust Fluid Catalytic Cracking (FCC) Riser Reactor Model", Petroleum Training Journal, Vol.4, NO.1, P.36-51
- Jacob S. H., Gross B, Voltz S. E. and Weekman V. M. (1976). "A Lumping and Reaction Scheme for Catalytic Cracking", AIChE Journal, 22, 701-713.
- Jose Roberto Hernandez-Barajas, Richart Vazquez-Roman, Ma. G. Felix-Flores (2009), "A comprehensive estimation of kinetic parameters in lumped catalytic cracking reaction models", Fuel, Volume 88, P.169-178
- Jafar S. Ahari, Amir Farshi and Khaled Forsat (2008), "A Mathematical Modeling of the riser Reactor in Industrial FCC Unit, Petroleum and Coal 50 (2) 15-24.
- Port Harcourt Refinery Company (PHRC) Project (1987). "Nigerian National Petroleum Corporation Process", 12<sup>th</sup> June 1987, Project No. 9465A- Area 3 FCCU 16, P.1-205.
- Rajkumar Gupta, Vineet Kumar, and V.K. Srivastava (2005). Modeling and simulation of fluid catalytic cracking unit. Reviews in Chemical Engineering, Vol. 21, No. 2, 95-131.

Versteeg H. K. and Malalasekera W., "An Introduction to Computational Fluid Dynamics, the Finite Volume Method", 2<sup>nd</sup> Edition, Pearson Educational Limited, England (2007).

Ying L., Qing T., and Rodney O.F., "CFD Modelling of Chemical Reactors: Single-Phase Complex Reactions and Fine-Particle Production", Department of Chemical and Biological Engineering, Iowa State University, IA 50010-2230, U.S.A., E-mail:liuying@iastate.edu (2006).

Yousuo D. And Ogbeide S.E. (2015). A Comparative Study of Different Kinetic Lumps Model in the Fluid Catalytic Cracking Unit Using COMSOL Multiphysics, Petroleum science and Technology, 33:2, 159-169, DOI: 10.1080/10916466.2014.958237. [Online]. Available <http://dx.doi.org/10.1080/10916466.2014.958237> (April 30, 2015)

## Nomenclature

The nomenclature is given in table 8.

**Table 1: Boundary conditions**

SETTINGS	BOUNDARY	BOUNDARY	BOUNDARIES
	3	4	1 and 2
<b>Temperature</b>			
Boundary type	Inlet	Outlet	wall
Boundary condition	Temperature	Temperature	Thermal insulation
Value	T <sub>0</sub>	T <sub>n</sub>	-
<b>Concentration</b>			
Boundary type	Inlet	Outlet	wall
Boundary condition	Concentration	Concentration	Insulation/Symmetry
Value	c <sub>in</sub> for all species	c <sub>out</sub> for all species	-
<b>Velocity and pressure</b>			
Boundary type	Inlet	Outlet	Wall
Boundary condition	Velocity	Pressure, no viscous stress	No slip
Value	w <sub>0</sub> =v <sub>s</sub> , u <sub>0</sub> =v <sub>0</sub> =0	P <sub>0</sub> =P-n	-

**Table 2: Riser dimensions**

	Length (m)	Diameter ((m)
Riser reactor	33	0.8

**Table 3: Average molecular weight and heat capacities (Jafar et al, 2008)**

Species	MW (kg/kmol)	Cp (kJ/kg.K)
Gas oil	333.0	2.67(liquid), 3.3(Gas)
Gasoline	106.7	3.3
Light gases	40.0	3.3
Coke	14.4	1.087
Steam	18.0	1.9
Catalyst	N/A	1.087

**Table 4: Thermodynamic properties of the feed**

Gas oil vaporization temperature	698K
Viscosity of gas	1.4 x 10 <sup>-3</sup> N.S/m <sup>2</sup>
Gas oil enthalpy of vapourisation	190 kJ/kg

**Table 5: PHRC plant operating conditions (PHRC, 1987)**

Feed rate (kg/s)	30.87
Feed Quality (API)	D1298
COR (kg/kg)	7.04
Inlet pressure (kPa)	221
Feed temperature (K)	505
Catalyst inlet temperature (K)	1004
Steam (wt%)	5
Steam temperature (K)	464
Catalyst density (kg m <sup>-3</sup> )	840
Gas density (kg m <sup>-3</sup> )	5.3
Gas velocity (m sec <sup>-1</sup> )	2.5

**Table 6: Kinetic data for the cracking reactions (Rajkumar et al., 2005)**

Cracking Reaction	Activation energy (kJ/mol)	Frequency factor (hr <sup>-1</sup> )	Rate at 538 <sup>o</sup> C (hr <sup>-1</sup> )	Molecular weight of cracking lump
HFO to LFO	60.7086	1.422 x 10 <sup>7</sup>	1760.4	380
HFO to gasoline	23.0274	1.026 x 10 <sup>5</sup>	3380.4	380
HFO to coke	73.269	3.704 x 10 <sup>7</sup>	712.8	380
LFO to gasoline	23.0274	8.215 x 10 <sup>4</sup>	2707.2	255
LFO to coke	73.269	1.852 x 10 <sup>7</sup>	356.4	255
Gasoline to coke	41.868	8.555 X 10 <sup>4</sup>	172.8	120
Gas oil to gasoline	68.2495	7.978 x 10 <sup>5</sup>	39.364	380
Gas oil to gas	89.2164	4.549 x 10 <sup>6</sup>	9.749	380
Gas oil to coke	64.5750	3.765 x 10 <sup>4</sup>	6.012	380
Gasoline to gas	52.7184	3.255 x 10 <sup>3</sup>	2.470	120
Gasoline to coke	115.4580	7.957 x 10 <sup>1</sup>	1.364	120

**Table 7: Kinetic lumps, Predicted values and deviation of predicted values from the practical values**

	PHRC PLANT	Predicted	Deviation
Gasoline yield, (wt %)	49.50	51	1.5
Coke yield, (wt %)	5.90	6.25	0.35
Outlet Temperature, (K)	805	803	-2

**Table 8: Nomenclature**

c: Concentration, mol/m <sup>3</sup>	M <sub>cat</sub> (M <sub>cat</sub> ): Mass flow rate of catalyst, kg/s
E: Activation energy for rate constant, J/mol	P <sub>in</sub> : Inlet pressure, pa
g: Acceleration due to gravity, m/s <sup>2</sup>	R <sub>g</sub> (R <sub>u</sub> ): Gas constant, J/(mol.K)
P: The pressure of gases, pa	T <sub>cat</sub> : Temperature of the catalyst, K
R, r: Rate expression value	ε: Void fraction
T: Temperature, K	T <sub>go</sub> : Temperature of gas oil, K
t, τ: Residence time, s	T <sub>vap</sub> : Gas oil vapourization temperature, K
v: Volume, m <sup>3</sup>	v <sub>0</sub> : Outlet velocity, m/s
z: Axial distance from the inlet, m	T <sub>ds</sub> : Temperature of the steam, K
CP <sub>cat</sub> (C <sub>p</sub> <sub>cat</sub> ): Specific heat of catalyst, J/kgK	V <sub>R</sub> , v, V: Reactor volume, m <sup>3</sup>
Cp <sub>ds</sub> (C <sub>p</sub> <sub>ds</sub> ): Specific heat of steam, J/kgK	W <sub>s</sub> : Additional work term
Cp <sub>L_GO</sub> (C <sub>p</sub> <sup>L<sub>go</sub>): Specific heat of liquid gas oil, J/kgK</sup>	Q: Heat due to chemical reaction, J/m <sup>3</sup> .s
Cp <sub>V_GO</sub> (C <sub>p</sub> <sup>V<sub>go</sub>): Specific heat of gaseous gas oil, J/kgK</sup>	Q <sub>ext</sub> : Heat added to the system, J/m <sup>3</sup> .s
C <sub>i</sub> : Species molar concentrations, mol/m <sup>3</sup>	μ: Viscosity, N.S/m <sup>2</sup>
c <sub>in</sub> : Inlet concentration, mol/m <sup>3</sup>	ρ: Density, Kg/m <sup>3</sup>
c <sub>out</sub> : Outlet concentration, mol/m <sup>3</sup>	Ψ: Slip fact
K <sub>d</sub> : Deactivation constant	<b>Subscripts</b>
M <sub>go</sub> (M <sub>go</sub> ): Mass flow rate of gas oil, kg/s	j: Refers to lump j that is cracked
M <sub>ds</sub> (M <sub>ds</sub> ): Mass flow rate of steam, kg/s	i: Refers to lump i that is formed
	p (or s): Particle/solid
	a (or f): Air/fluid
	cat: Catalyst
	c: Coke content

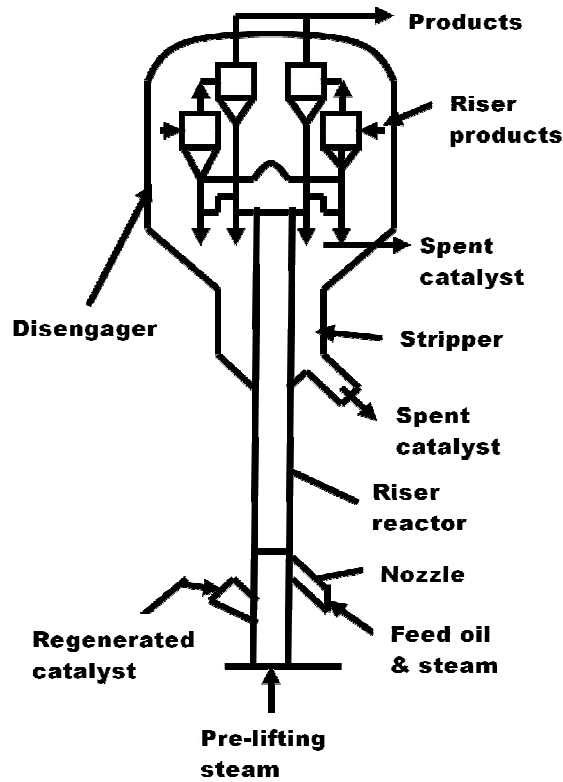


Figure 1: The PHRC FCC reactor

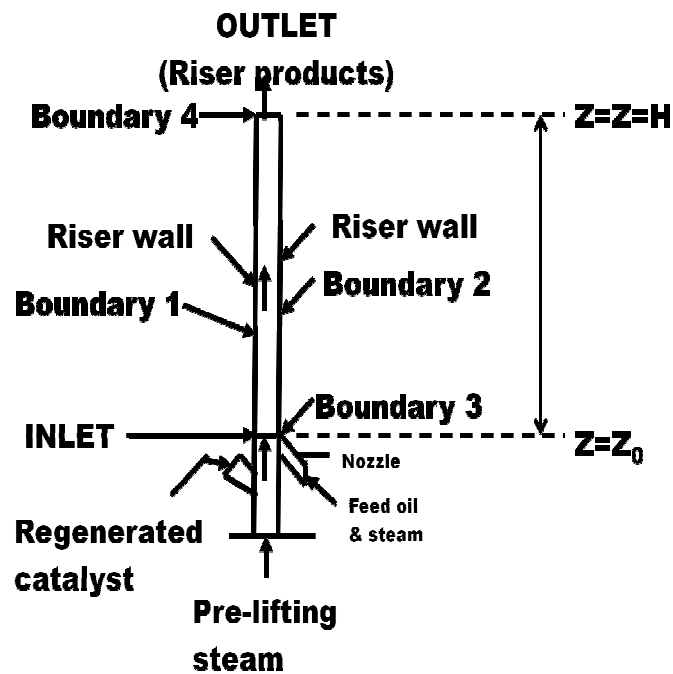


Figure 2: The PHRC FCC riser reactor

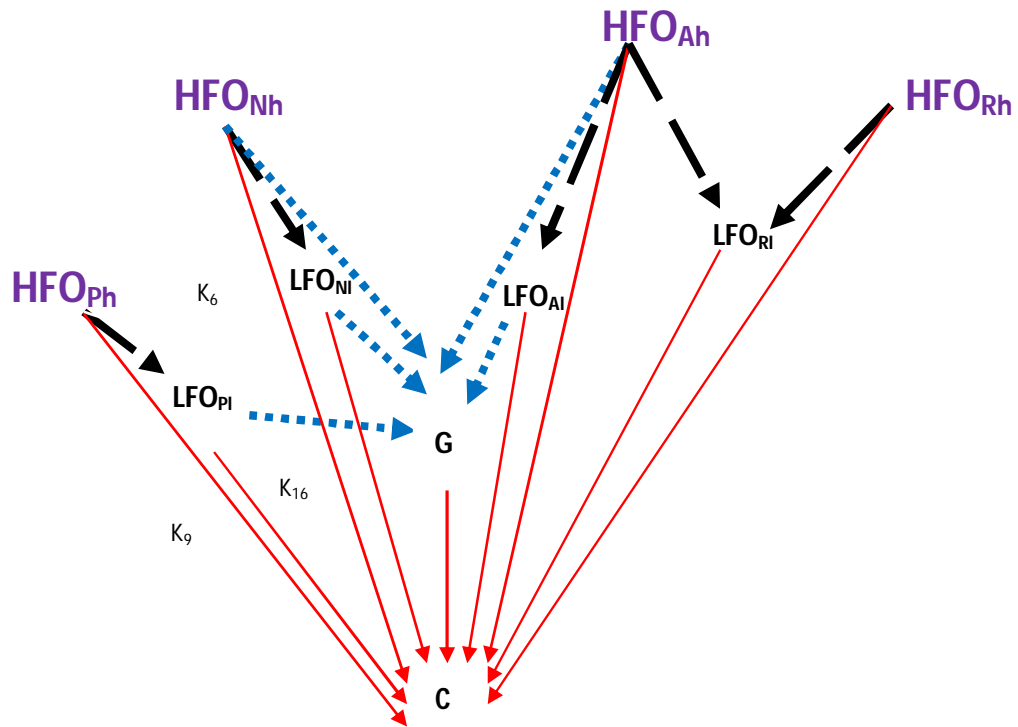


Figure 3: Ten-Lump Kinetic scheme .

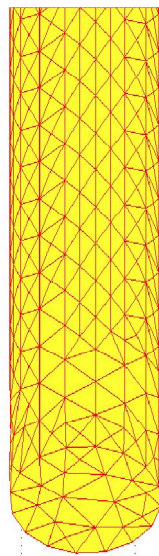


Figure 4: Computational domain and grid used in the simulation study of a section of the riser from the bottom

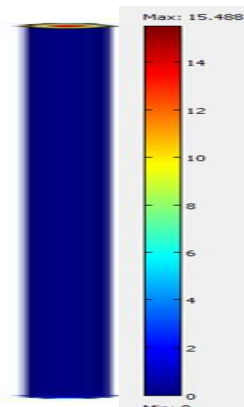


Figure 5. The distribution of surface velocity in the riser

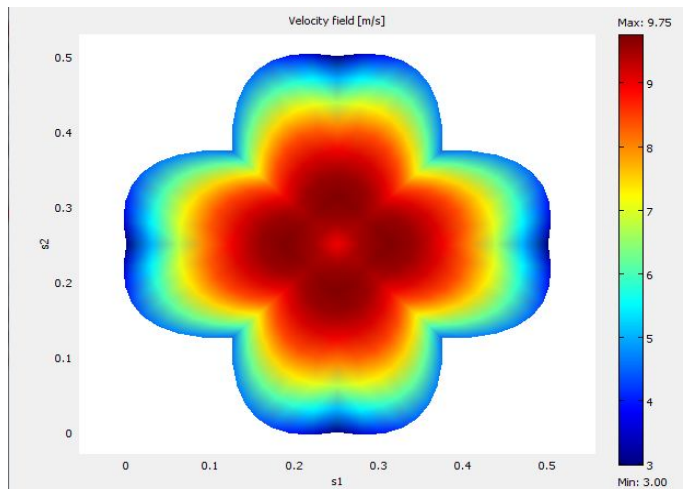


Figure 6. The surface velocity at the input of the riser reactor

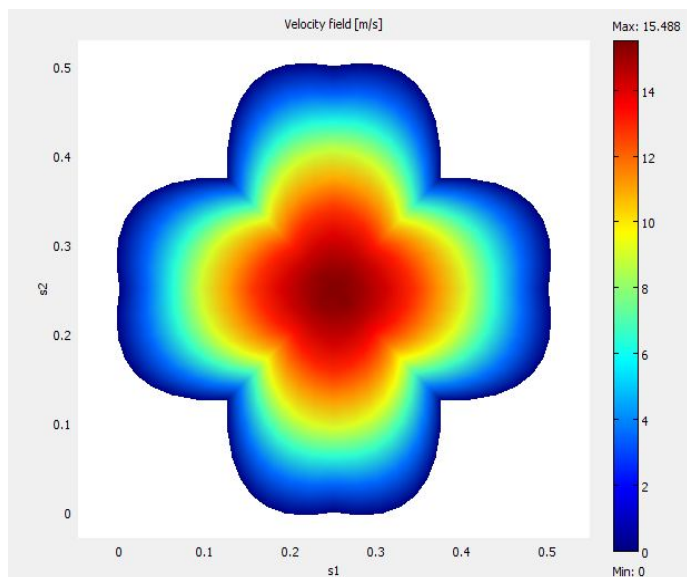


Figure 7. The surface velocity at the output of the riser reactor

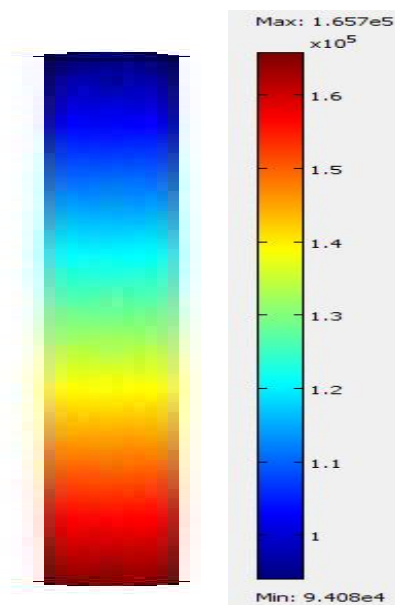


Figure 8 The distribution of surface pressure in the riser

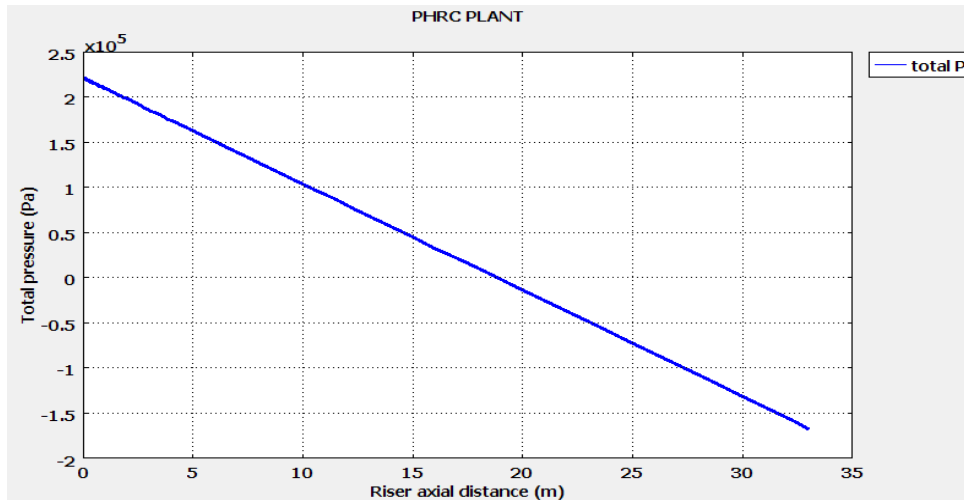


Figure 9. The pressure in the reactor riser versus riser axial distance

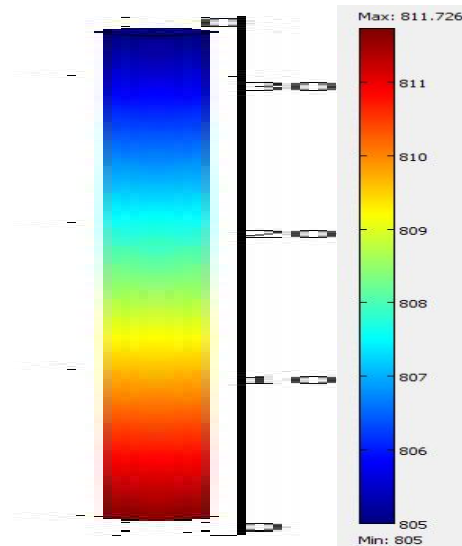


Figure 10. The temperature profile in the reactor riser

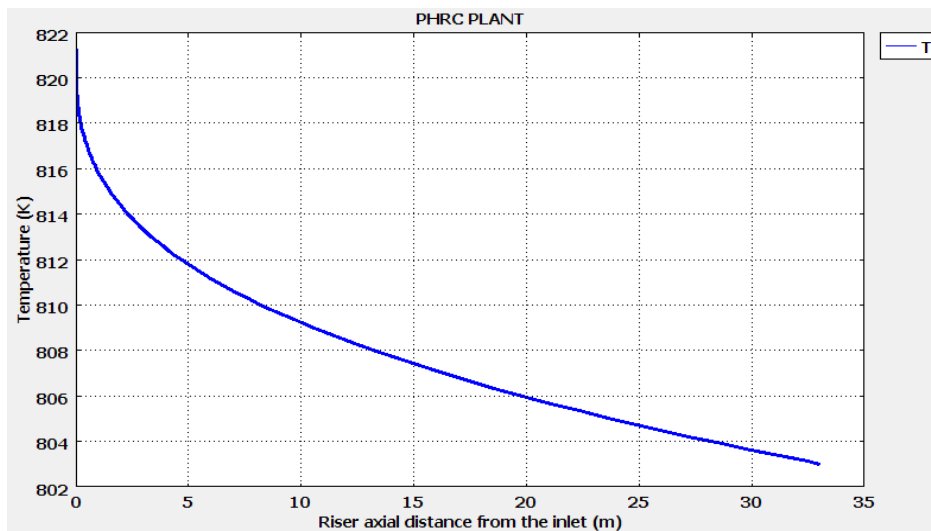


Figure 11. The temperature in the reactor riser versus riser axial distance (PHRC plant)

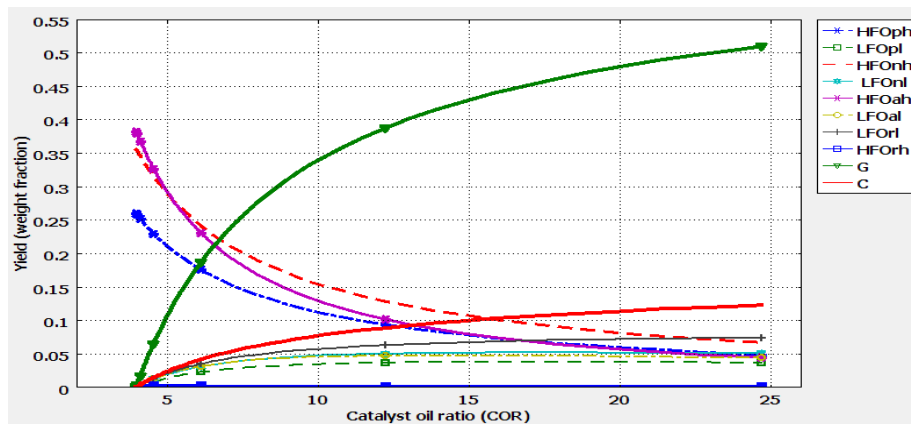


Figure 12. The effect of catalyst oil ratio (COR) on yield.

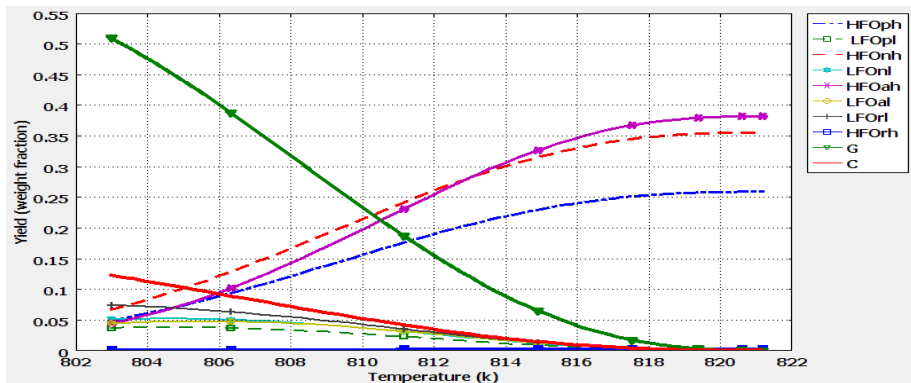


Figure 13. The effect of changing inlet temperature on yield.

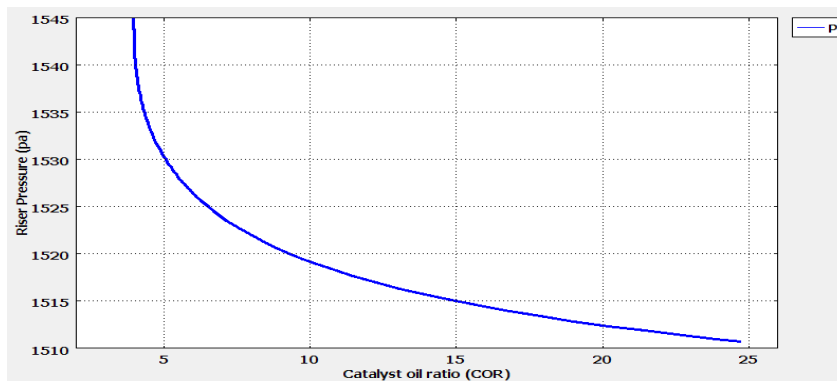


Fig 14. The riser pressure versus catalyst oil ratio (COR)

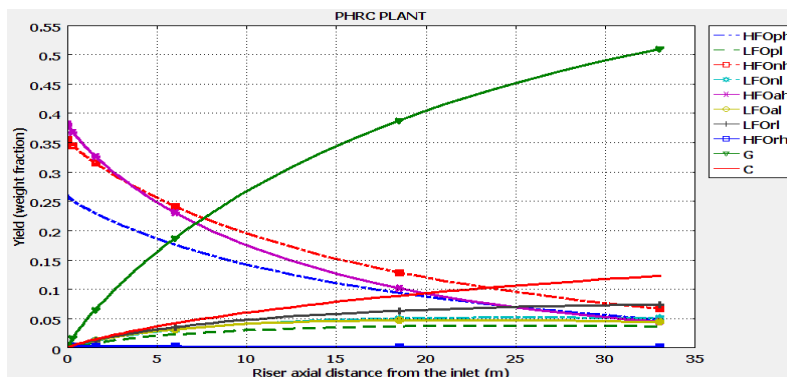


Figure 15. The yield in the reactor riser versus riser axial distance